

## Enhanced Photochromism of Heteropolyacid/Polyvinylpyrrolidone Composite Film by TiO<sub>2</sub> Doping

Cong Lu,<sup>1</sup> Yan Sun,<sup>1</sup> Jialu Liu,<sup>1</sup> Xiansheng Wang,<sup>1</sup> Su-Ling Liu,<sup>2</sup> Wei Feng<sup>1</sup>

<sup>1</sup>Key Lab of Groundwater Resources and Environment, Ministry of Education, Jilin University, 2519 Jie Fang Road, 130021, Changchun, China

<sup>2</sup>Key Laboratory of Industrial Ecology and Environmental Engineering, MOE, School of Environmental Science and Technology, Dalian University of Technology, Dalian 116024, China

Correspondence to: W. Feng (E-mail: weifeng@jlu.edu.cn)

**ABSTRACT:** Novel composite film was synthesized by TiO<sub>2</sub> doping into phosphomolybdic acid (PMoA)/polyvinylpyrrolidone (PVP) system. The influence of TiO<sub>2</sub> doping on its microstructure and photochromic properties was investigated via atomic force microscopy, transmission electron microscope, Fourier transform infrared spectroscopy (FT-IR), ultraviolet–visible spectra, and X-ray photoelectron spectroscopy (XPS). After TiO<sub>2</sub> doping, the surface of TiO<sub>2</sub>/PMoA/PVP composite film changed to rough from smooth, and the particle size significantly increased. The FT-IR results verified that the basic structure of PMoA and PVP were not destroyed in the composite films. The non-bonded interaction between the acid and polymer was strengthened by TiO<sub>2</sub> doping. Irradiated with UV light, composite films changed from colorless to blue. The TiO<sub>2</sub>/PMoA/PVP composite film exhibited a strong photochromic effect and faster bleaching reaction than that of PMoA/PVP film. XPS results indicated that the amount of PMoA in photo-reductive reaction was increased after TiO<sub>2</sub> doping, which resulted in the photochromic efficiencies enhanced. © 2014 Wiley Periodicals, Inc. *J. Appl. Polym. Sci.* **2015**, *132*, 41583.

**KEYWORDS:** photochromic performance; polyoxometalates; polyvinylpyrrolidone; TiO<sub>2</sub> doping

Received 4 June 2014; accepted 28 September 2014

DOI: 10.1002/app.41583

### INTRODUCTION

Photochromic materials have been widely used as building materials due to their novel properties such as heat insulation, radiation protection, energy saving, and decoration.<sup>1,2</sup> Polyoxometalates (POMs) is a series of molecularly defined inorganic metal-oxide clusters<sup>3</sup> and can accept one or more electrons to yield mixed-valency colored species (e.g., heteropolyblues), which makes them suitable as photochromic, thermochromic, and electrochromic materials.<sup>4,5</sup> However, it is difficult to manipulate the structural, physical, and chemical properties of POMs in practical application.

Subsequently, it was found that entrapping POMs nanoparticles into polymeric network can provide good mechanical properties, conferring high kinetic stability on POMs nanoparticles. Moreover, some photochromic materials prepared by embedding POMs into polymer matrix via hydrogen bond or chemical bond exhibited great physical and chemical properties of composites. Therefore, polymer not only acts as dispersion matrix but also as electrons donator of the photo-reductive reaction in

the POMs/polymer system. Recently, some polymers with active group such as polyacrylamide (PAM),<sup>6–8</sup> polyvinylpyrrolidone (PVP),<sup>9</sup> polyvinyl alcohol (PVA),<sup>10–12</sup> and polyether chains (PEs)<sup>13–15</sup> have been successfully applied to synthesize special structure and cost-effective photochromic composites.

As discussed above, interaction between different components had significant effect on the microstructure and photochromic properties of composite materials. Thus, adding the third functional phase into two-phase composite system has become a hot issue in composites field.<sup>16–18</sup> TiO<sub>2</sub> would be of interest due to its high photo-oxidation activity, chemical stability, and non-toxicity, etc. in photochemistry.<sup>19</sup> Specifically, TiO<sub>2</sub> can provide electron to induce the reduction of heteropolyacids (heteropolyblues generated) in the photochemical reaction,<sup>20</sup> which may enhance the photochromic properties of composites. In view of that, the primary objectives of this study are to prepare new phosphomolybdate acid (PMoA)/ PVP composite film with TiO<sub>2</sub> doping and to investigate the microstructure, photochromic properties, and mechanisms of TiO<sub>2</sub>/PMoA/PVP composite

Additional Supporting Information may be found in the online version of this article.

© 2014 Wiley Periodicals, Inc.

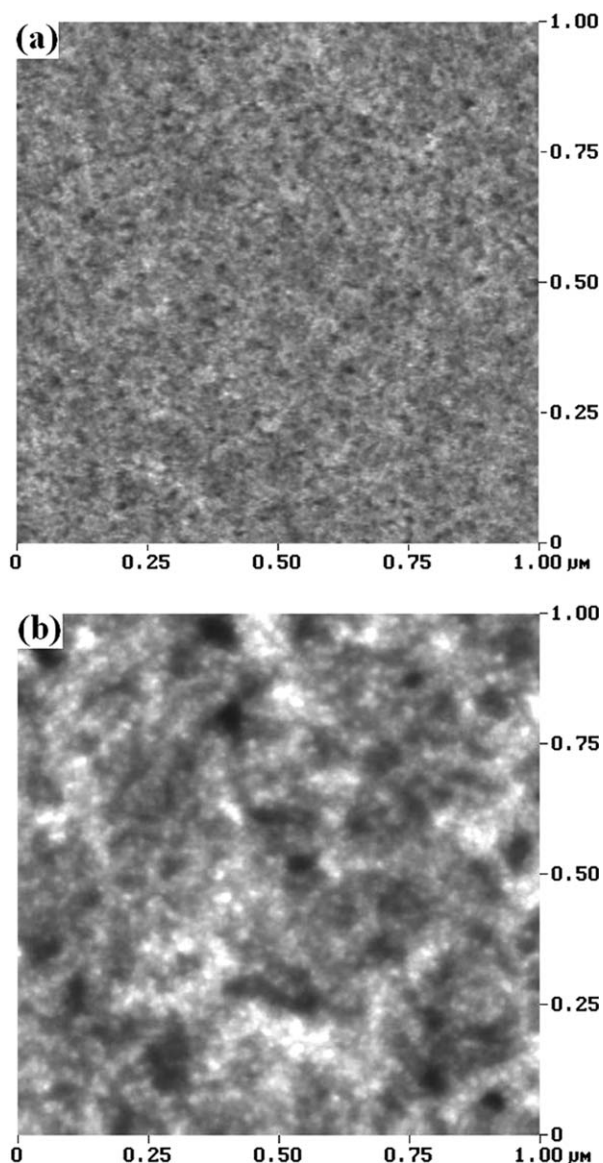


**Figure 1.** AFM images of (a) PMoA/PVP and (b) TiO<sub>2</sub>/PMoA/PVP composite film.

film. Experimental results indicated that the photochromic property was enhanced by the addition of TiO<sub>2</sub>.

## EXPERIMENTAL

### Materials

Keggin type PMoA was purchased from Tianjin Kermel Chemical Reagent Development Center and purified by recrystallizing twice. PVP ( $M_w$  50,000) was obtained from Aldrich and purified by fractional distillation before use. Tetrabutyl titanate was purchased from ShenYang Chemical Reagent. All other chemicals used in this study were of analytical grade and deionized water was used in all experiments.

### Preparation

About 2 mL *N*-butyl titanate was dissolved in the 10 mL absolute ethanol by slowly stirring for 30 minutes. Then 2 mL acetic acid and 0.7 mL triethanolamine were added to the *N*-butyl

titanate solution. After 1 h of stirring, 10 mL absolute ethanol and 0.2 mL deionized water was gradually added to the mixed solution for 1 h stirring till shallow yellow transparent sol was obtained. Then, 0.5 mL acetylacetone was added to the transparent sol with 30 minutes stirring. Finally, the transparent TiO<sub>2</sub> colloidal suspension was obtained after 24 h ageing. Some characteristics for TiO<sub>2</sub> colloidal suspension such as content, size, and shape of TiO<sub>2</sub> nanoparticles and zeta potential are shown in the Supporting Information. TiO<sub>2</sub> nanoparticles, whose content was 7.2% in colloidal suspension were sphere with the size of 15 nm (see Figure S1 in Supporting Information). The TiO<sub>2</sub> colloidal suspension was stable in the pH range of 2–6.9 and the zeta potential decreased with the increase of pH value (see Figure S2 in Supporting Information). The zero zeta potential point appeared at 6.9 of pH value, and TiO<sub>2</sub> colloidal suspension became condensed or flocculated at this point due to the Coulombian force.

PMoA and PVP were dissolved in ethanol with a concentration of 10 mg/mL, respectively. Then 2 mL PMoA solution was slowly dripped into the 2 mL PVP solution for 2 h reaction to get transparent solution. After that, 200  $\mu$ L TiO<sub>2</sub> colloidal suspension was slowly dripped into PMoA/PVP solution till transparent composite solution was obtained. Finally, PMoA/PVP and TiO<sub>2</sub>/PMoA/PVP composite film were prepared by dripping the transparent solution on various substrates such as silicon (the size was 5  $\times$  5 mm), KBr plates (the diameter was 5 mm), copper grid (the diameter was 1 mm), and quartz plates (the size was 15  $\times$  8 mm), which were used for atomic force microscopy (AFM) studies, Fourier transform infrared spectroscopy (FT-IR), transmission electron microscope (TEM) studies, and ultraviolet–visible (UV–vis) spectroscopy, respectively. All films were dried in a chamber with controlled air humidity that did not exceed 60% in order to obtain optically perfect film. In this study, the thickness of the film was approximately 2.1  $\mu$ m, which was measured by a FCT-1030 Film Thickness Measurement System (LCD Lab, Changchun Institute of Optics, Fine Mechanics and Physics, Chinese Academy of Science).

### Instrumental Analysis

AFM images were tested in air atmosphere using the (Auto Probe CP) AFM in non-contact mode. TEM observations were performed on a JEOL JEM-2100, operating at 200 kV, in order to identify the microstructure of composite films. FT-IR spectra were determined by samples deposited on KBr pellets at room temperature with a Nicolet Impact 550 FT-IR spectrometer in the range of 4000–400  $\text{cm}^{-1}$ . Absorbance curves were measured on an UV–vis spectrophotometer (JASCO V-550) with 1 nm optical resolution in the range of 350–900 nm. X-ray photoelectron spectroscopy (XPS) valence band spectra were obtained with ESCA LAB-MKII photoelectron spectrometer.

**Table I.** Roughness Results of PMoA/PVP and TiO<sub>2</sub>/PMoA/PVP Film

Film	Scanning area ( $\mu\text{m}^2$ )	$R_a$ (nm)	RSM (nm)
PMoA/PVP	5 $\mu\text{m} \times 5 \mu\text{m}$	15.6	21.4
TiO <sub>2</sub> /PMoA/PVP		20.3	34.5

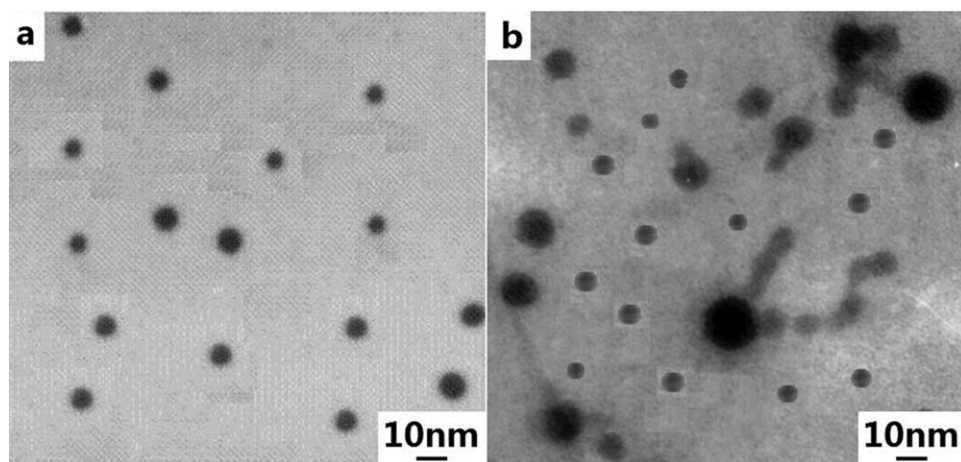


**Figure 2.** TEM images of (a) PMoA/PVP and (b) TiO<sub>2</sub>/PMoA/PVP composite film (The big sphere was TiO<sub>2</sub> particles and the small sphere was PMoA particles).

Photochromic experiments were carried out using a 500 W high-pressure mercury lamp as the light source. The distance between the lamp and films was 150 mm. Films were exposed to air during the process of UV irradiation. After irradiation for a certain time, *in situ* absorbance curve was obtained. The irradiation time was recorded until the curve was just the same as the before one. Films were sheltered from light under air conditions and the absorption spectra were measured at regular intervals to monitor the bleaching process. All measurements were carried out at room temperature.

## RESULTS AND DISCUSSION

### AFM Measurements

To reveal the change of surface morphology before and after TiO<sub>2</sub> doping, AFM images of PMoA/PVP and TiO<sub>2</sub>/PMoA/PVP composite films were illustrated in Figure 1. For PMoA/PVP composite film, the regular rolling mountain peaks with similar size were observed over the surface [see Figure 1(a)]. After TiO<sub>2</sub> doping, the surface of TiO<sub>2</sub>/PMoA/PVP composite film changed rough from smooth and exhibited similar spherical shape with nonuniform size [see Figure 1(b)]. Film surface roughness was also determined using AFM images (Table I). Compared with PMoA/PVP film, the surface roughness of TiO<sub>2</sub>/PMoA/PVP composite film was apparently increased. The root-mean-squared (RMS) surface roughness and the mean surface roughness (Ra) increased from 21.4 and 15.6 nm to 34.5 and 20.3 nm, respectively.

### TEM Measurements

The microstructure of PMoA/PVP and TiO<sub>2</sub>/PMoA/PVP composite films is observed by TEM images [Figure 2(a,b)]. The PMoA particles, with average diameter of 7 nm, exhibited regular spherical shape and dispersed uniformly in PMoA/PVP composite films. The TiO<sub>2</sub> particles with the size of 15 nm dispersed uniformly in the composite films after TiO<sub>2</sub> doping and the size and shape of PMoA particles have no change, as shown in Figure 2(b). This result was in accord with AFM.

### FT-IR Spectra

FT-IR spectra of PMoA/PVP and TiO<sub>2</sub>/PMoA/PVP composite films before and after UV irradiation in the range of 500–

3500 cm<sup>-1</sup> were illustrated in Figure 3. For comparison, pure PVP and PMoA in KBr pellet were also given.

Generally, the vibration bands at 1650–1684 cm<sup>-1</sup> (C=O group), 1280 cm<sup>-1</sup> (C–N group), and 2905–2968 cm<sup>-1</sup> (C–H group) were attributed to the organic groups of PVP.

For the PMoA/PVP and TiO<sub>2</sub>/PMoA/PVP composite films, the characteristic vibration bands [ $\nu(\text{C}=\text{O})$ ,  $\nu(\text{C}-\text{N})$ ,  $\nu(\text{C}-\text{H})$ ] of PVP still existed and had a few cm<sup>-1</sup> shifts [see Figure 3(b–d)], indicating that the basic structure of PVP undestroyed. In the FT-IR spectra of pure Keggin type PMoA, there were four characteristic bands representing the Keggin structure at 1062, 962, 870, and 783 cm<sup>-1</sup> assigned to stretching vibration  $\nu(\text{P}-\text{O}_a)$ ,  $\nu(\text{Mo}-\text{O}_d)$ ,  $\nu(\text{Mo}-\text{O}_b-\text{Mo})$ , and  $\nu(\text{Mo}-\text{O}_c-\text{Mo})$ , respectively.<sup>21</sup> In this study, those characteristic vibration bands possessed in the composite films [Figure 3(c,d)] were similar to those of pure PMoA except for a shift of a few cm<sup>-1</sup>, which suggested that the Keggin geometry of PMoA was still preserved and the strong interfacial interaction between PMoA and PVP was built inside the composite films.

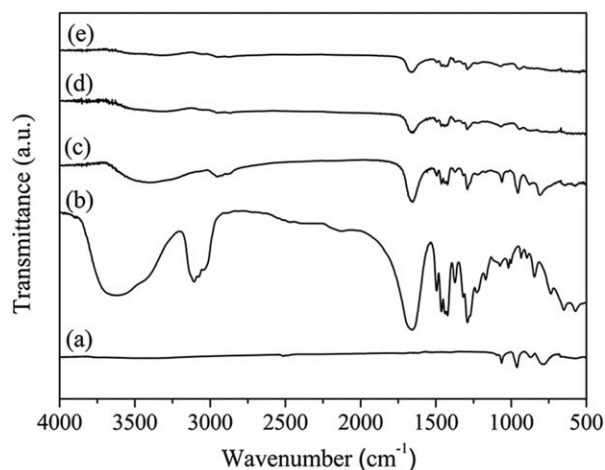


**Figure 3.** FT-IR spectra of (a) PMoA, (b) PVP, (c) PMoA/PVP, TiO<sub>2</sub>/PMoA/PVP composite film (d) before and (e) after UV irradiation.

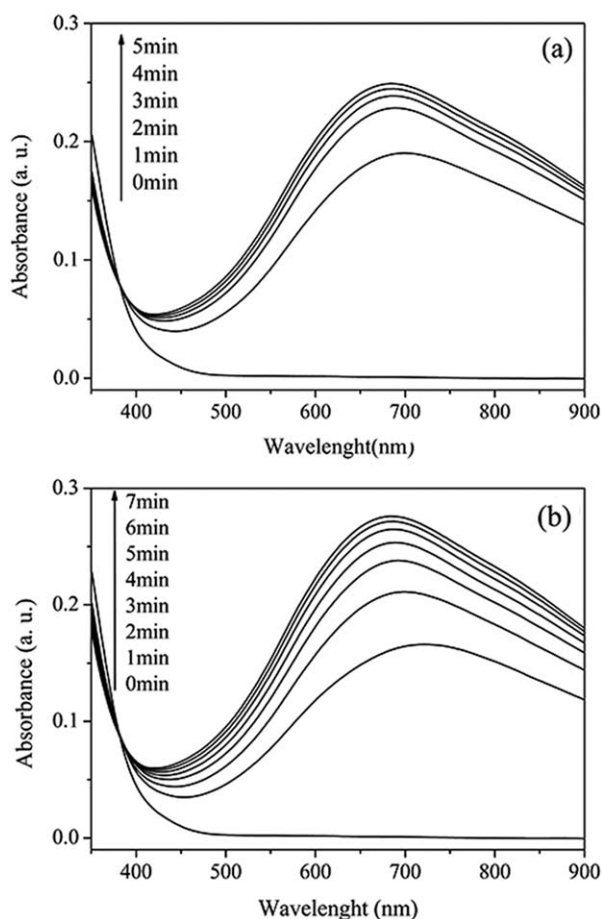


**Figure 4.** UV-vis adsorption spectra of (a) PMoA/PVP and (b) TiO<sub>2</sub>/PMoA/PVP composite film.

Additionally, the  $\nu(\text{P-O}_a)$  band had no change due to having no impact on the P-O<sub>a</sub> vibration after TiO<sub>2</sub> added. The Mo-O<sub>d</sub> vibration was considered as a pure stretching one, whose vibration wave-number was an increasing function of anion-anion interaction.<sup>22</sup> Comparing with PMoA/PVP composite film [Figure 3(c)], the Mo-O<sub>d</sub> asymmetrical stretching frequency of TiO<sub>2</sub>/PMoA/PVP composite film [Figure 3(d)] had a blue shift by 11 cm<sup>-1</sup>. This was attributed to the influence of TiO<sub>2</sub>, which led to the increasing of the anion-anion distance and the weakening of anion-anion electrostatic interaction. Because  $\nu(\text{Mo-O}_b\text{-Mo})$  and  $\nu(\text{Mo-O}_c\text{-Mo})$  vibrations were not pure stretching and cannot be free from bending character, there was a competition of opposing effects. The electrostatic anion-anion interaction led to an increase of the frequencies of vibrations. So the Mo-O<sub>b</sub>-Mo and Mo-O<sub>c</sub>-Mo bands can be used to evaluate the interactions between organic and inorganic components. While TiO<sub>2</sub> was added into the film,  $\nu(\text{Mo-O}_b\text{-Mo})$  and  $\nu(\text{Mo-O}_c\text{-Mo})$  all had blue shifts by 6 and 4 cm<sup>-1</sup>, respectively, illustrating the strengthening of non-bonded interaction between anion and polymer-cation. After UV irradiation, the Mo-O<sub>b</sub>-Mo and Mo-O<sub>c</sub>-Mo vibration in the TiO<sub>2</sub>/PMoA/PVP composite film still had a few red shifts [Figure 3(e)], proving that the heteropolyacids accepting electrons was transformed to be heteropolyblues and correspondingly the colorless composite film turned to blue.

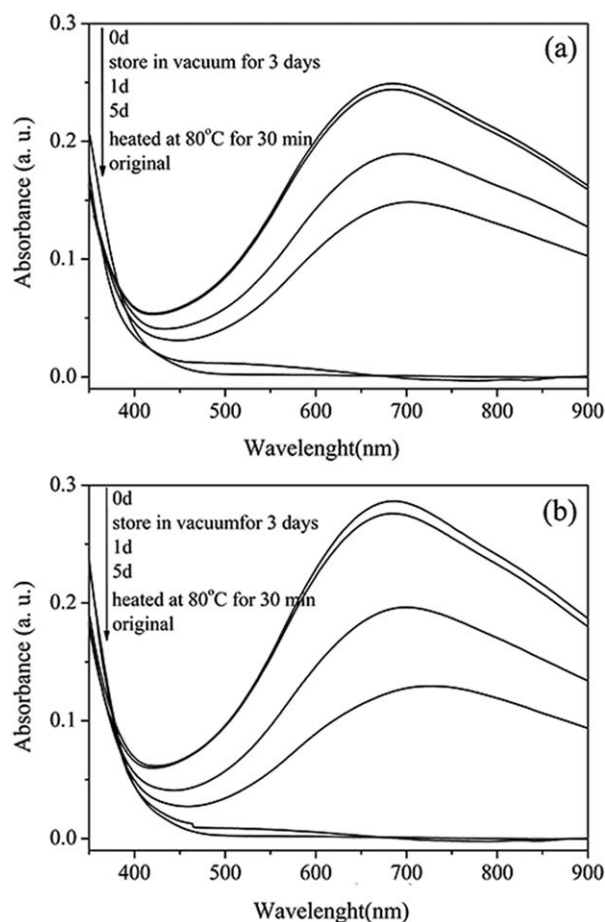


**Figure 5.** UV-vis absorption spectra of (a) PMoA/PVP and (b) TiO<sub>2</sub>/PMoA/PVP composite film with different bleaching process.

### Photochromic Properties

The UV-vis absorption spectra of PMoA/PVP and TiO<sub>2</sub>/PMoA/PVP composite films with different UV irradiation time were investigated in this study (Figure 4). Before UV irradiation, there was no significant absorption of PMoA/PVP and TiO<sub>2</sub>/PMoA/PVP composite films in UV-vis region. After UV

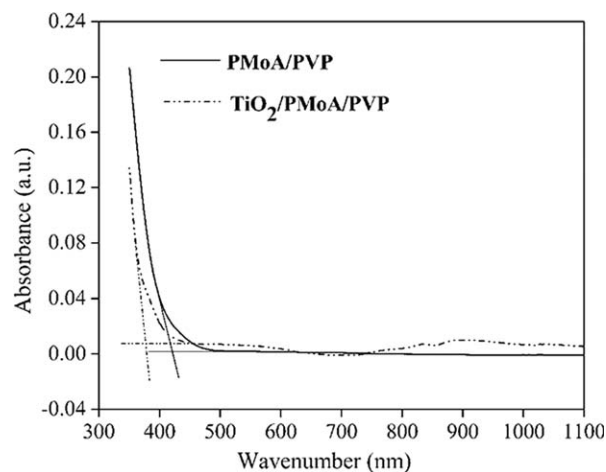


**Figure 6.** UV absorbance edge of PMoA/PVP and TiO<sub>2</sub>/PMoA/PVP composite film.

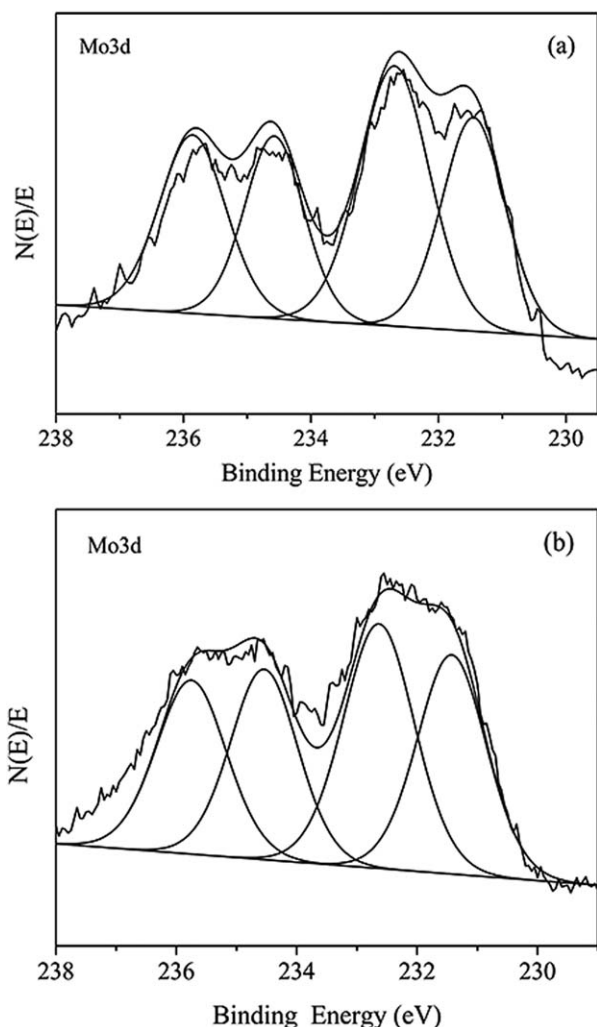


**Figure 7.** Gaussian deconvolution of  $\text{Mo}_{3d}$  level spectra of (a) PMoA/PVP and (b)  $\text{TiO}_2/\text{PMoA}/\text{PVP}$  composite film for 10 minutes UV irradiation.

irradiation, the colorless composite film turned to blue and appeared one characteristic band at 720–750 nm which were attributed to  $\text{Mo}^{6+} \rightarrow \text{Mo}^{5+}$  intervalence charge transfer (IVCT).<sup>23</sup> The intensity enhanced and the position of the maximum IVCT underwent a blue shift with increasing irradiation time. The absolute absorbency of PMoA/PVP and  $\text{TiO}_2/\text{PMoA}/\text{PVP}$  composite films was increased as irradiation time prolonged and saturated after UV irradiated for 5 and 7 minutes, respectively. After 5 minutes UV irradiation at 680 nm, the absorbance intensity of PMoA/PVP composite film was 0.249, while the absorbance intensity of  $\text{TiO}_2/\text{PMoA}/\text{PVP}$  was 0.276 under the same condition. It showed that  $\text{TiO}_2/\text{PMoA}/\text{PVP}$

hybrid film showed a stronger photochromic effect and increased light absorption efficiency of the composite film.

The bleaching process of PMoA/PVP and  $\text{TiO}_2/\text{PMoA}/\text{PVP}$  composite films is familiar, as shown in Figure 5. After visible light had been turned off, films began to bleach gradually in air. If the irradiated hybrid films are stored in nitrogen or vacuum conditions, the color of hybrid films would remain for 3 days. When changing the ambient atmosphere to air or oxygen, the bleaching process took place. The results showed that oxygen played an important role during the bleaching process. Contrasting Figure 5(a,b), it was found that the bleaching speed of  $\text{TiO}_2/\text{PMoA}/\text{PVP}$  film was faster than that of PMoA/PVP film. The bleaching speed is controlled by the diffusion and transmission rate of oxygen in the composites. From AFM images, the surface of  $\text{TiO}_2/\text{PMoA}/\text{PVP}$  film was rougher than that of PMoA/PVP film, which was conducive to the transmission of oxygen. Thus it is relatively easy to carry the oxidation reaction process of heteropolyblues. When the hybrid films were heated at 80°C in air for 30 minutes, the color-change of films turned back its original color, indicating that heat accelerated the bleaching process of composite films.

#### Mechanism

Band gap of UV absorbance edge can give a great understanding of the optical response of the composite films. Figure 6 showed the UV absorbance edge of PMoA/PVP and  $\text{TiO}_2/\text{PMoA}/\text{PVP}$  composite films before UV irradiation in the range of 350–900 nm, which reflected the influence of doping  $\text{TiO}_2$  on the optical properties.

The absorption edge of  $\text{TiO}_2/\text{PMoA}/\text{PVP}$  composite film had a blue shift from 420 to 377 nm comparing to PMoA/PVP film and the shifting of optical response of  $\text{TiO}_2/\text{PMoA}/\text{PVP}$  to ultraviolet region could well be understood from the decrease in the band gap value from 2.95 to 3.28 eV. The result indicated the available energy of proton would improve by the addition of  $\text{TiO}_2$ , which potentially enhanced the photochromic performance of composite with UV irradiation.

XPS spectra were used to investigate the influence of  $\text{TiO}_2$  on the variation of electronic structure of the composite films during the photochromic process so as to make clear the effect of mechanism of  $\text{TiO}_2$  [as shown in Figure 7(a,b)]. Through Gaussian deconvolution,  $\text{Mo}_{3d}$  spectra of PMoA/PVP and  $\text{TiO}_2/\text{PMoA}/\text{PVP}$  composite films could be well resolved into  $3d_{5/2}$  and  $3d_{7/2}$  doublet caused by spin-orbit and the binding energies (BE) are listed in Table II. The  $\text{Mo}_{3d}$  doublet of  $\text{Mo}^{6+}$  and the  $\text{Mo}_{3d}$  doublet of  $\text{Mo}^{5+}$  were all detected in the PMoA/PVP and  $\text{TiO}_2/\text{PMoA}/\text{PVP}$  composite films, which indicated that the photo-reductive reaction took place after UV irradiation and

**Table II.** Binding Energies (eV) of  $\text{Mo}_{3d}$  of PMoA/PVP and  $\text{TiO}_2/\text{PMoA}/\text{PVP}$  Composite Film After 10 Minutes UV Irradiation

Sample	$\text{Mo}^{5+}$		$\text{Mo}^{6+}$		$\text{Mo}^{5+}/\text{Mo}$ ratios
	$3d_{5/2}$	$3d_{7/2}$	$3d_{5/2}$	$3d_{7/2}$	
PMoA/PVP	231.45	234.58	232.69	235.86	0.45
$\text{TiO}_2/\text{PMoA}/\text{PVP}$	231.40	234.55	232.65	235.75	0.51

consequently heteropolyblues was generated. For TiO<sub>2</sub>/PMoA/PVP composite film, the BE values of Mo<sub>3d</sub> double peak of Mo<sup>6+</sup> were 232.65 and 235.75 eV and those of Mo<sup>5+</sup> were 231.40 and 234.55 eV, which were lower than the values of PMoA/PVP composite films. Evidently, the different binding energy in TiO<sub>2</sub>/PMoA/PVP presented a different reductive valence state during the photo-reduction process, which indicated that the chemical microenvironment of Mo was changed. Besides, two chemical valences' degenerate peak areas via the XPS spectra were calculated by integral operation to provide the photo-reductive reaction extent. The results in this study showed that Mo<sup>5+</sup>/Mo ratio of TiO<sub>2</sub>/PMoA/PVP composite film was significant higher than that of PMoA/PVP composite film (in Table II), corresponding to the stronger photochromic properties under the same irradiation condition. Generally, the results demonstrated that TiO<sub>2</sub> was involved in the photo-reductive reaction, consequently enhancing the photo-reduction extent of heteropolyacids.

## CONCLUSION

Novel photochromic composite film was prepared by doping TiO<sub>2</sub> into PMoA/PVP composite film. The TiO<sub>2</sub> doping had a great effect on the microstructure and photochromic properties of composite film. The surface morphology of composite film changed from smooth to rough with regular spherical shape. The addition of TiO<sub>2</sub> enhanced the photochromic performance of composite film, which was related to the participation of TiO<sub>2</sub> changed the interaction between PMoA and PVP matrix.

## ACKNOWLEDGMENTS

The present work was funded by the National Science Foundation Committee projects of China (Grant No. 61340048; Grant No. 41302182), the Specialized Research Fund for the Doctoral Program of Higher Education of China (Grant No.20110041120001) and Industrial Technology Research and Development projects in Jilin province (Grant No.2013C044).

## REFERENCES

1. Feng, W.; Ding, Y. S.; Liu, Y.; Lu, R. *Mater. Chem. Phys.* **2006**, *98*, 347.
2. Yao, J. N.; Hashimoto, K.; Fujishima, A. *Nature* **1992**, *355*, 624.
3. Pope, M. T. *Heteropoly and Isopoly Polyoxometalates*, Springer-Verlag: Berlin, **1983**.
4. Yamase, T. *Chem. Rev.* **1998**, *98*, 307.
5. Nakane, K.; Yamashita, T.; Iwakura, K.; Suzuki, F. *J. Appl. Polym. Sci.* **1999**, *74*, 133.
6. Feng, W.; Zhang, T. R.; Liu, Y.; Lu, R.; Zhao, Y. Y.; Li, T. J.; Yao, J. N. *J. Solid State Chem.* **2002**, *169*, 1.
7. Feng, W.; Zhang, T. R.; Liu, Y.; Wei, L.; Lu, R.; Li, T. J.; Zhao, Y. Y.; Yao, J. N. *J. Mater. Res.* **2002**, *17*, 133.
8. Bao, X. J.; Feng, W.; Chen, J.; Liu, X. Y. *J. Solid State Chem.* **2012**, *191*, 158.
9. Zhang, T. R.; Lu, R.; Liu, X. L.; Zhao, Y. Y.; Li, T. J.; Yao, J. N. *J. Solid State Chem.* **2003**, *172*, 458.
10. Gong, J.; Li, X. D.; Shao, C. L.; Ding, B.; Lee, D. R.; Kim, H. Y. *Mater. Chem. Phys.* **2003**, *79*, 87.
11. Chen, J.; Ai, L. M.; Feng, W.; Xiong, D. Q.; Liu, Y.; Cai, W. M. *Mater. Lett.* **2007**, *61*, 5247.
12. Ai, L. M.; Feng, W.; Chen, J.; Liu, Y.; Cai, W. M. *Mater. Chem. Phys.* **2008**, *109*, 131.
13. Judeinstein, P.; Oliveira, P. W.; Krug, H.; Schmidt, H. *Chem. Phys. Lett.* **1994**, *220*, 35.
14. Judeinstein, P.; Oliveira, P. W.; Krug, H.; Schmidt, H. *Adv. Mater. Opt. Electr.* **1997**, *7*, 123.
15. Mo, Y. G.; Dillon, R. O.; Snyder, P. G.; Tiwald, T. E. *Thin Solid Films* **1999**, *355–356*, 1.
16. Wang, Z. L.; Ma, Y.; Zhang, R. L.; Xu, D.; Fu, H. B.; Yao, J. N. *J. Solid State Chem.* **2009**, *182*, 983.
17. Russo, M.; Rigby, S. E. J.; Caserin, W.; Stingelin, N. *J. Mater. Chem.* **2010**, *20*, 1348.
18. Chen, J.; Liu, S. L.; Feng, W.; Bao, X. J.; Yang, F. L. *Opt. Mater.* **2013**, *35*, 973.
19. Chen, Y. X.; Wang, K.; Lou, L. P. *J. Photochem. Photobiol. A* **2004**, *163*, 281.
20. Qi, H.; Liu, Y.; Feng, W.; Zhu, Y. *Sci. China Ser. B* **2009**, *52*, 169.
21. Sanchez, C.; Soler-Illia, G. J. D. A.; Ribot, E.; Lalot, T.; Mayer, C. R.; Cabuil, V. *Chem. Mater.* **2001**, *13*, 3061.
22. Checkiewicz, K.; Zukowska, G.; Wiczorek, W. *Chem. Mater.* **2001**, *13*, 379.
23. Papaconstantinou, E. *Chem. Soc. Rev.* **1989**, *18*, 1.